SCIENCE CHINA
Information Sciences

• **Supplementary File** •

Joint-decoding-complexity-oriented Collaborative Design for Joint Source-Channel Coding System Based on Double Protograph-LDPC Codes

Zhiping Xu[1], Dan Song[2], Jiachun Zheng[1] & Lin Wang[2*]

[1]*Xiamen Key Laboratory of Marine Intelligent Terminal R&D and Application, the School of Ocean Information Engineering, Jimei University, Xiamen* 361021*, P. R. China;*
[2]*Department of information and Communication Engineering, Xiamen University, Xiamen* 361005*, P. R. China*

Appendix A Background

Joint source-channel coding (JSCC) systems have attracted increasing attention owing to the effective utilization of the residual redundancy from the source coding [1]- [3]. Among these systems, the JSCC system based on double low-density parity-check (LDPC) codes, named D-LDPC JSCC system, can achieve better performance due to its joint Tanner structure [1]. As a variant of D-LDPC JSCC system, JSCC system based on double protograph LDPC (DP-LDPC) codes [4]- [12], named DP-LDPC JSCC system, utilizes the protograph LDPC (P-LDPC) codes as its element codes, and the P-LDPC codes have simple and fast encoding structure [20]- [23]. The researches on DP-LDPC JSCC system mainly focus on the different kinds design over the standard/non-standard coding channel. Here, standard coding channel is defined as the combination of BPSK modulation and the additive white Gaussian noise (AWGN) channel, and the other combinations of non-BPSK modulation and complex channels are defined as non-standard coding channels [12].

In the standard coding channel, a lot of efforts have been devoted to studying the DP-LDPC JSCC system with single-element optimization or multi-elements optimization in the joint base matrix. In respect to the single-element optimization, the source code is optimized to get the lower error-floor [4], and an unequal power allocation strategy through the optimization of source code is used to improve the performance [5]. The channel code is redesigned to obtain better performance of the water-fall region [6]. The optimization methods for the edge connection between source code and channel code are developed [7], [8]. In the regard of multi-elements optimization, the source code and channel code are jointly optimized to improve the performance over the AWGN channel [9], [11]. Moreover, a joint shuffled scheduling decoding algorithm was proposed for DP-LDPC JSCC system to lower decoding complexity [19].

In the non-standard coding channel, many complex factors need to be considered in the optimization process, such as channel statistic matching, modulation matching. In the aspect of channel statistic matching, the non-standard coding channel, including M-ary differential chaos shift keying (M-DCSK) [13] and Rayleigh fading channels, was considered in [12] firstly. In this work, the easy channel statistic was considered. And then, complex channel statistic was considered in [28] and a numerical Gaussian approximation method was proposed to solve the complex channel whose channel statistic is non-Gaussian-like distribution. Furthermore, a probabilistic amplitude shaping method was proposed for DP-LDPC JSCC system [29], where matching between the probability distribution of the modulated symbols and the row degree distribution of source code was investigated.

From these works concluded above, it can be seen that the code optimization works in this system are devoted to improve performance without considering the constraint of the decoding complexity, which is an important property in the decoding side and crucial for real applications. In the tandem separated source-channel coding (SSCC) system, the decoding complexity can be estimated to be $\mathcal{O}(EI_{max})$, where E represents the sum of nonzero entries in the parity-check matrix (PCM) and I_{max} represents the maximum decoding iterations [14]- [17]. The iteration numbers are limited to optimize the irregular LDPC codes by numerical design methods [14], and the protograph extrinsic information transfer (PEXIT) [24] analysis is limited by the iteration numbers to obtain P-LDPC codes with low decoding complexity [15], [16]. The number of nonzero entries in PCM is taken into consideration to analyze the decoding complexity [17]. Decreasing computational complexity in one iteration decoding process is an efficient method to reduce decoding complexity [27]. When the sum of the nonzero entries in PCM decreases, both the computational complexity and the decoding complexity can be reduced.

In the existing research on the DP-LDPC JSCC system, I_{max} is always set to a high value in the code optimization process, such as 100 [9] or 200 [10], which will lead to high decoding complexity. One may wonder if previously designed code pairs will still perform well when decoding complexity, becomes an important constraint in the process of code design. As of today, how to design the DP-LDPC JSCC system with low decoding complexity is an open question. Moreover, no matter in standard or non-standard coding channels, the optimization of coding and decoding sides in the DP-LDPC JSCC system are separated considered. The superiority of collaborative design has been verified in the SSCC system [30], but how to realize the collaborative design framework for the DP-LDPC JSCC system is still another open question.

Appendix B System Model

In the DP-LDPC JSCC system, a joint base matrix $\mathbf{B}_J$ of size $(m_{\rm sc}+m_{\rm cc})\times(n_{\rm sc}+n_{\rm cc})$ is defined as

* Corresponding author (email: wanglin@xmu.edu.cn)

$$\mathbf{B}_J = \begin{bmatrix} \mathbf{B}_{sc} & \mathbf{B}_{L1} \\ \mathbf{B}_{L2} & \mathbf{B}_{cc} \end{bmatrix}, \tag{B1}$$

where $\mathbf{B}_{sc}$ is the base matrix of source P-LDPC code of size $m_{\rm sc} \times n_{\rm sc}$, $\mathbf{B}_{cc}$ is the base matrix of channel P-LDPC code of size $m_{\rm sc} \times n_{\rm sc}$, $\mathbf{B}_{L1}$ represents the edges connecting the check nodes (CNs) of the source P-LDPC code to the variable nodes (VNs) of the channel P-LDPC code in the joint Tanner graph of size $m_{\rm sc} \times n_{\rm cc}$, and $\mathbf{B}_{L2}$ represents the edges connecting the CNs of channel P-LDPC code to the VNs of the source P-LDPC code in the Tanner graph of size $m_{\rm cc} \times n_{\rm sc}$.

In order to obtain the joint parity check matrix $\mathbf{H}_J$, the operation of "copy-and-permute" is implemented by the progressive edge growth (PEG) algorithm [25] with a lifted factor q, which will remove the parallel edges from the base matrix of the P-LDPC codes. The joint parity-check matrix of size $(M_{\rm sc} + M_{\rm cc}) \times (N_{\rm sc} + N_{\rm cc})$, corresponding to the joint base matrix $\mathbf{B}_J$, is defined as

$$\mathbf{H}_J = \begin{bmatrix} \mathbf{H}_{sc} & \mathbf{H}_{L1} \\ \mathbf{H}_{L2} & \mathbf{H}_{cc} \end{bmatrix}, \tag{B2}$$

where $\mathbf{H}_{sc}$ is the parity check matrix of source P-LDPC code of size $M_{sc} \times N_{sc}$, $\mathbf{H}_{cc}$ is the parity check matrix of channel P-LDPC code of size $M_{cc} \times N_{cc}$, and $\mathbf{H}_{L1}$ and $\mathbf{H}_{L2}$ are the linking matrixes between these two P-LDPC codes.

Fig. B1 shows the system model. Let $\boldsymbol{m}$ be the source sequence, generated by a binary i.i.d Bernoulli source with entropy $H(\boldsymbol{m}) = -p_m \log_2(p_m) - (1-p_m)\log_2(1-p_m)$, where p_m is the probability of "1" and $p_m \neq 0.5$. In the encoder, the source sequence $\boldsymbol{m}$ is compressed into the sequence $\boldsymbol{s} = \boldsymbol{m} \cdot \mathbf{H}_{sc}^T$. Then, another P-LDPC code, which is defined by $\mathbf{H}_{cc}^{new} = [\mathbf{H}_{L2} \quad \mathbf{H}_{cc}]$, is used to realize error control coding, and the systematic generator matrix of $\mathbf{H}_{cc}^{new}$ will be denoted by $\mathbf{G}_{cc}^{new}$. The codeword sequence $\boldsymbol{c}$ is generated by $\boldsymbol{c} = \boldsymbol{s}^{new} \cdot \mathbf{G}_{cc}^{new}$, where $\boldsymbol{s}^{new} = [\boldsymbol{m}_p, \boldsymbol{s}]$ and $\boldsymbol{m}_p$ is the part of $\boldsymbol{m}$ connected to the check nodes of the channel codes. Next, the generated sequence $\boldsymbol{c}$ is modulated to sequence $\boldsymbol{y}$ by binary phase shift keying (BPSK), and then the sequence $\boldsymbol{y}$ is transmitted over an AWGN channel. In the receiver, the sequence $\boldsymbol{z}$, which is the corrupted version of the sequence $\boldsymbol{y}$, is passed onto the joint decoder.

As depicted in Fig. B2, the joint decoder consists of source decoder and channel decoder. The belief propagation (BP) algorithm is used in the joint decoder to obtain the evaluated sequence $\hat{\boldsymbol{m}}$, while the source statistics are considered at the same time. The extrinsic messages between source and channel decoders are exchanged through the edges between two decoders in the joint Tanner graph.

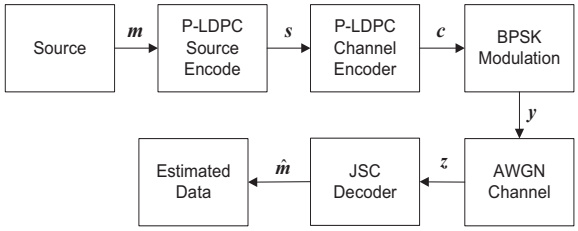

Figure B1 Model of the DP-LDPC JSCC system.

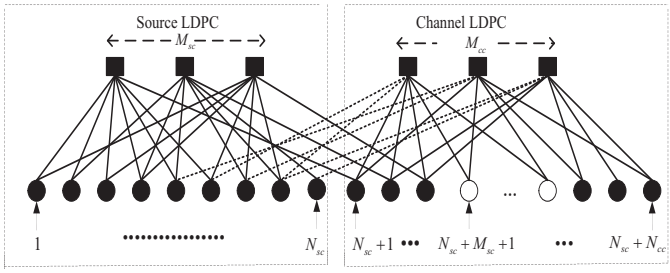

Figure B2 Joint decoder of the DP-LDPC JSCC system

Appendix C Collaborative Design Based on Joint Decoding Complexity

Appendix C.1 The Definition of Joint Decoding Complexity

Following [17]- [19], the joint decoding complexity of the DP-LDPC JSCC system (denoted by **JDC**) is defined by

$$\begin{aligned} \mathbf{JDC} &\propto E \cdot I_{max} \\ &= Sum(\mathbf{H}_J) \cdot I_{max} \\ &= Sum(\mathbf{H}_{sc} + \mathbf{H}_{cc} + \mathbf{H}_{L1} + \mathbf{H}_{L2}) \cdot I_{max} \\ &= Sum(\mathbf{B}_{sc} \cdot q_{sc} + \mathbf{B}_{cc} \cdot q_{cc} + \mathbf{B}_{L1} \cdot q_1 + \mathbf{B}_{L2} \cdot q_2) \cdot I_{max}, \end{aligned} \tag{C1}$$

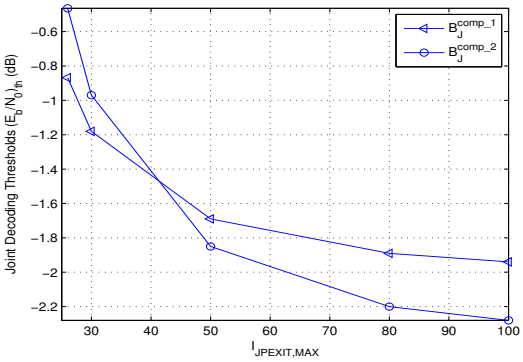

Figure C1 The joint decoding thresholds under different maximum iteration numbers when $p_m = 0.04$.

where $Sum(\mathbf{H}_J)$ represents the sum of entries in the joint parity-check matrix of this system and I_{max} represents the maximum iteration numbers. As mentioned before, $\mathbf{H}_J$ consists of four parts: $\mathbf{H}_{sc}$, $\mathbf{H}_{cc}$, $\mathbf{H}_{L1}$ and $\mathbf{H}_{L2}$. And they are obtained from $\mathbf{B}_{sc}$, $\mathbf{B}_{cc}$, $\mathbf{B}_{L1}$ and $\mathbf{B}_{L2}$ by lifting operation with lifting factor q_{sc}, q_{cc}, q_1 and q_2, respectively [6]. Generally, $q_{sc} = q_{cc} = q_1 = q_2$.

The matrix $\mathbf{B}_J$ includes four components: $\mathbf{B}_{sc}$, $\mathbf{B}_{cc}$, $\mathbf{B}_{L1}$ and $\mathbf{B}_{L2}$. In order to accelerate the design process, some components of $\mathbf{B}_J$ can be fixed to reduce the code searching space. In the DP-LDPC JSCC system, the performance of the water-fall region is mainly influenced by channel codes [6]. In this paper, the main concern is to improve the performance of the water-fall region with low joint decoding complexity, and the focus will be on the redesign of channel code under this constraint. Recall, the work in [10] is the latest work for DP-LDPC JSCC system without considering the decoding complexity so far. Hence, $\mathbf{B}_{sc}$ in $\mathbf{B}_J$ is fixed to be that of $\mathbf{B}_J^{opti\_2}$ from Eq. (17) in [10], denoted as $\mathbf{B}_{sc}^{fix}$, in the following work. $\mathbf{B}_{L1}$ is fixed to the connection between the check CNs of the channel code and the VNs with a larger degree of the source code [7]. Let $\mathbf{B}_{L2} = \mathbf{0}$ in this paper, because it has no effect on the design of channel P-LDPC code. Since the three components are fixed, $Sum(\mathbf{B}_J)$ is determined by $Sum(\mathbf{B}_{cc})$.

Appendix C.2 Analysis with Limited Iteration Number

For the convenience of expression, the optimal channel base matrix corresponding to Eq. (16) and Eq. (17) in [10] are denoted as $\mathbf{B}_{cc}^{comp\_1}$ and $\mathbf{B}_{cc}^{comp\_2}$, respectively. The code pairs $(\mathbf{B}_{sc}^{fix}, \mathbf{B}_{cc}^{comp\_1})$ and $(\mathbf{B}_{sc}^{fix}, \mathbf{B}_{cc}^{comp\_2})$ are denoted as $\mathbf{B}_J^{comp\_1}$ and $\mathbf{B}_J^{comp\_2}$, respectively. I_{max}^{JPEXIT} represents the maximum iteration numbers in the JPEXIT analysis [10]. The impact of I_{max}^{JPEXIT} on joint decoding thresholds, denoted as $(E_b/N_0)_{th}$, is shown in Fig. C1.

It can be seen that the $(E_b/N_0)_{th}$ with $I_{max}^{\text{JPEXIT}} = 100$ of $\mathbf{B}_J^{comp\_2}$ outperforms the $(E_b/N_0)_{th}$ with $I_{max}^{\text{JPEXIT}} = 25$ and $I_{max}^{\text{JPEXIT}} = 30$ by 1.8dB and 1.3dB, respectively. When $I_{max}^{\text{JPEXIT}} = 100$, $\mathbf{B}_J^{comp\_2}$ has 0.3dB coding gain, compared to $\mathbf{B}_J^{comp\_1}$. But, when $I_{max}^{\text{JPEXIT}} = 25$, $\mathbf{B}_J^{comp\_2}$ is worse than $\mathbf{B}_J^{comp\_1}$, for there is 0.3dB gap between them. The impact of the maximum iteration number is summarized as follows.

(i) The joint decoding threshold is affected to a greater degree by the maximum iteration number. The smaller the maximum iteration number, the higher the joint decoding threshold.

(ii) The channel code optimized by specific maximum iteration number may not always perform well with another maximum iteration number.

Therefore, the channel code of the DP-LDPC JSCC system needs to be redesigned, taking into consideration the maximum iteration number.

Appendix C.3 The Collaborative Design Process for the Channel Code of DP-LDPC JSCC

The Collaborative Design Process for the Channel Code of DP-LDPC JSCC with low joint decoding complexity can be formulated as an optimization problem, with the objective function considering the maximum iteration number, as follows:

$$\min_{\mathbf{B}_J} \quad \boldsymbol{\theta}\left(\mathbf{B}_J, I_{max}^{\text{JPEXIT}}\right), \tag{C2}$$

$$\mathbf{s.t.} \qquad \mathscr{F}_t\left(\mathbf{B}_J\right) \geqslant 0, \quad t = 1, 2, \ldots, T, \tag{C3}$$

where the function $\boldsymbol{\theta}\left(\mathbf{B}_J, I_{max}^{\text{JPEXIT}}\right)$ returns the joint decoding thresholds of $\mathbf{B}_J$ by JPEXIT analysis with the limitation of I_{max}^{JPEXIT}. Ineq. (C3) represents the design constraints for the channel code of the DP-LDPC JSCC system. In order to design channel code for the DP-LDPC JSCC system with low joint decoding complexity, there are many constraints to be considered, and specific constraints are summarized as follows.

(a) Low channel decoding threshold

Based on [20], a good protograph is the combination of one or more degree-1 VNs, one very high degree VN, and several degree-2 VNs. When the puncturing operation is allowed, puncturing the highest degree VN will achieve better performance.

(b) Linear minimum distance growth

The maximum number of degree-2 VNs in the tandem SSCC system of the protograph, denoted by n_1, can be calculated by $m_{cc} - m_p - 1$ [20]. In the DP-LDPC JSCC system, the maximum number of degree-2 VNs, denoted by n_2, can be calculated by $m_{cc} + m_{sc} - m_p - 1$ [11], where m_p is the number of precoder structures (degree-1 VNs). In the new design, we set the maximum number of degree-2 VNs in the interval $[n_1, n_2]$.

(c) Decoding complexity

From Eq. (C1), the decoding complexity can be represented by the sum of entries in the joint base matrix and the maximum number of the iteration. The smaller the sum of entries and maximum iterations, the lower the decoding complexity.

(d) Search complexity and optimized space

The size of the joint base matrix is directly related with the search complexity. The smaller the size, the lower the search complexity. But, the space of the good codes is also limited by its size; the smaller the size, the smaller the space that can be optimized. One has to make a tradeoff between search complexity and optimized space.

The design of a rate-1/2 channel code is considered here, and $\mathbf{B}_{cc}^{comp\_2}$ is used for performance comparison. The size of $\mathbf{B}_{cc}^{comp\_2}$ is 3×5 and this restricts the optimized space. In order to make a tradeoff between search complexity and the optimized space, the protograph is set as a 6×10 matrix, which is the same as $\mathbf{B}_{cc}^{comp\_2}$ when the PEG algorithm performed with $q = 2$. Considering the constraint conditions mentioned before, the initial channel base matrix is set as

$$\mathbf{B}_{cc,1}^{(0)} = \begin{bmatrix} 1 & 0 & 0 & 0 & 0 & b_{1,6} & b_{1,7} & b_{1,8} & b_{1,9} & b_{1,10} \\ 0 & 1 & 0 & 0 & 0 & b_{2,6} & b_{2,7} & b_{2,8} & b_{2,9} & b_{2,10} \\ 0 & 0 & 1 & 1 & 0 & b_{3,6} & b_{3,7} & b_{3,8} & b_{3,9} & b_{3,10} \\ 0 & 0 & 0 & 0 & 1 & b_{4,6} & b_{4,7} & b_{4,8} & b_{4,9} & b_{4,10} \\ 0 & 0 & 1 & 0 & 0 & b_{5,6} & b_{5,7} & b_{5,8} & b_{5,9} & b_{5,10} \\ 0 & 0 & 0 & 1 & 1 & b_{6,6} & b_{6,7} & b_{6,8} & b_{6,9} & b_{6,10} \end{bmatrix}, \tag{C4}$$

where $b_{i,j}$ belongs to $\{0, 1, ..., e_p\}$ for $i = \{1, 2, ..., 6\}$ and $j = \{6, 7, ..., 10\}$, and e_p is the maximum value of each entry in the base matrix. The constraints mentioned previously for this base matrix are expressed as follows:

$$\begin{aligned} &\mathscr{F}_1 : \sum_{i_1=1}^{5} b_{i_1,j_1} - 3 \geqslant 0, \ j_1{=}k_1, k_2, ..., k_m, \forall k_m \in \{6, 7, ..., 10\}, \\ &\forall m \in \{3, 4, 5\}, k_1 \neq k_2 \neq ... \neq k_m. \end{aligned} \tag{C5}$$

$$\mathscr{F}_2 : \ Sum(\mathbf{B}_{cc}^{comp\_2} \times q) - Sum(\mathbf{B}_{cc}^{opt} \times q) \geqslant 0. \tag{C6}$$

$$\mathscr{F}_3 : 5 - \sum_{i_2=1}^{5} b_{i_2,j_2} \geqslant 0, \ j_2{=}\ 6, 7, ..., 10. \tag{C7}$$

The channel code with low joint decoding complexity searching is realized by a slightly modified genetic algorithm (GA) [9]. The steps are as follows.

GIVEN: The population number in one generation is N, the maximum generation number is G, the crossover probability is $p_{\rm cr}$, the mutation probability is $p_{\rm mt}$, the size of the candidate is S and $S = m_{cc} \times n_{cc}$.

INITIALIZATION: Generate $(N-1)$ candidates $\mathbb{P}_n^g$, $n = \{2, 3, ..., N\}$, which are replaced by the entries in $\mathbb{P}_1^g$ except those fixed entries, with values chosen from $\{0, 1, ..., e_p\}$ randomly. $\mathbb{P}_1^g = \mathbf{B}_{cc,1}^{(0)}$, $\mathbf{B}_{cc,\rm best}^{g-1} = \mathbf{B}_{cc,1}^{(0)}$. The initialization will continue until all $\mathbb{P}_n^g$ satisfy Eqs. (C5)-(C7).

CROSSOVER: For $n = \{1, 2, 3, ..., \frac{N}{2}\}$, randomly select $s_1, s_2 \in \{1, 2, ..., S\}$, $s_1 < s_2$. The crossover operation is conducted with probability $p_{\rm cr}$ as

$$\begin{cases} \mathbb{P}_{{\rm C},n+\frac{N}{2}}^g = \mathbb{P}_n^g(s_1, s_2). \\ \mathbb{P}_{{\rm C},n}^g = \mathbb{P}_{n+\frac{N}{2}}^g(s_1, s_2). \end{cases} \tag{C8}$$

MUTATION: For $n = \{1, 2, 3, ..., N\}$, $s = \{1, 2, 3, ..., S\}$, the mutation operation is conducted as

$$\mathbb{P}_{{\rm C},n}^g(s) = \begin{cases} b, \ b \in \{0, 1, ..., e_p\}, \quad with\ probability\ p_{\rm mt}. \\ \mathbb{P}_{{\rm C},n}^g(s), \ otherwise. \end{cases} \tag{C9}$$

SELECTION: For $n = \{1, 2, ..., N\}$ and $g = \{1, 2, ..., G\}$, the best candidate protograph in the g-th generation $\mathbb{P}_{\rm C,best}^g$ is chosen from $\mathbb{P}_{{\rm C},n}^g$, $n = \{1, 2, ..., N\}$, through the measure of objective function Eq. (C2):

$$\mathbf{B}_{cc,\rm best}^g(s) = \begin{cases} \mathbb{P}_{\rm best}^g \ if\ \boldsymbol{\theta}(\mathbb{P}_{\rm best}^{(g)}, I_{max}^{\rm JPEXIT}) < \\ \quad \boldsymbol{\theta}(\mathbf{B}_{cc,\rm best}^{(g-1)}, I_{max}^{\rm JPEXIT}), \\ \quad and\ \mathscr{F}_t \geqslant 0, \ t = 1, 2, 3. \\ \\ \quad \mathbf{B}_{cc,\rm best}^{(g-1)}, \ otherwise. \end{cases} \tag{C10}$$

TERMINATION: The operations of mutation and crossover are performed for G generations. The channel code, which has the lowest joint decoding threshold, will be chosen as the optimal result.

In order to limit the search complexity, e_p is set to 1. For other parameters, $N = 1000$; $G = 1000$; $p_{\rm cr} = 0.7$ and $p_{\rm mt} = 0.1$. Different values of these parameters can be chosen in the optimization procedure.

Using the above design method with the constraint conditions, the optimized rate-1/2 channel base matrix $\mathbf{B}_{cc}^{opt}$ with $I_{max}^{\rm JPEXIT}$=20 is obtained as

$$\mathbf{B}_{cc}^{opt} = \begin{bmatrix} 1 & 0 & 0 & 0 & 0 & 0 & 1 & 0 & 1 & 1 \\ 0 & 1 & 0 & 0 & 0 & 1 & 0 & 0 & 1 & 1 \\ 0 & 0 & 1 & 1 & 0 & 0 & 1 & 0 & 0 & 0 \\ 0 & 0 & 0 & 0 & 1 & 1 & 0 & 1 & 1 & 0 \\ 0 & 0 & 1 & 0 & 0 & 0 & 1 & 0 & 1 & 1 \\ 0 & 0 & 0 & 1 & 1 & 1 & 0 & 1 & 1 & 1 \end{bmatrix}. \tag{C11}$$

The joint base matrix corresponding to the code pair $(\mathbf{B}_{sc}^{fix}, \mathbf{B}_{cc}^{opt})$ is denoted as $\mathbf{B}_J^{opt}$. The joint decoding thresholds of $\mathbf{B}_J^{opt}$ under different maximum iteration numbers with $p_m = 0.04$ are shown in Table C1.

Table C1 Joint Decoding Thresholds of $\mathbf{B}_J^{opt}$ Under different Maximum Iteration Numbers at $p_m = 0.04$.

I_{max}^{JPEXIT}	25	30	50	80	100
$(E_b/N_0)_{th}$	-0.868	-1.181	-1.694	-1.894	-1.941

Table C2 Comparison of Joint Decoding Thresholds with $I_{max}^{\text{JPEXIT}} = 20$ at $p_m = 0.04$.

	B_J^{opt}	$\boldsymbol{B_J^{comp\_1}}$ [10]	$\boldsymbol{B_J^{comp\_2}}$ [10]
$(E_b/N_0)_{th}$	**-0.367**	-0.139	**0.282**

Appendix D Simulation Results

In this section, the simulation results of the proposed code are presented in two parts: performance comparisons over AWGN channel and Rayleigh fading channel [26], respectively. All simulations are written in C++ language using Visual Studio 2013. To guarantee a complete and fair performance comparison, the code pairs that satisfy and not satisfy the constraints of Eq. (C6) are analyzed. The frame length is set as 3200 bits, and the source statistic $p_m = 0.04$. The maximum iteration number I_{max} is set to 20. The label $(\mathbf{B}_J, I_{max})$ in the simulation figures means the scheme using $\mathbf{B}_J$ with I_{max} iterations. For example, $(\mathbf{B}_J^{opt}, 20)$ means this scheme using $\mathbf{B}_J^{opt}$ with $I_{max} = 20$.

Appendix D.1 Performance Comparisons over AWGN Channel

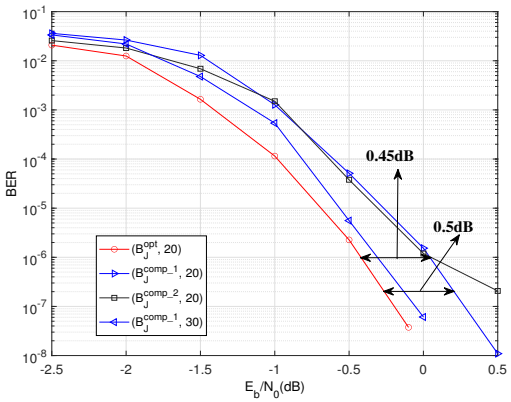

Figure D1 BER performance comparison at $p_m = 0.04$ over AWGN channel.

As shown in Fig. D1, the BER performance of $\mathbf{B}_J^{opt}$ at $p_m = 0.04$ has coding gains of 0.5dB at $BER = 2 \times 10^{-7}$ and 0.45dB at $BER = 1 \times 10^{-6}$ when $I_{max} = 20$, respectively, compared to $\mathbf{B}_J^{comp\_1}$ and $\mathbf{B}_J^{comp\_2}$, which are consistent with the joint decoding thresholds shown in Table C2. The BER curve of $\mathbf{B}_J^{comp\_1}$ with $I_{max} = 30$ is also presented in this figure. It can be observed that the BER performance of $\mathbf{B}_J^{comp\_1}$ with $I_{max} = 30$ is worse than that of $\mathbf{B}_J^{opt}$ with $I_{max} = 20$, and there are nearly 0.1dB gap between them. This means that one can reduce iteration numbers by nearly 33% $\left(\frac{30-20}{30}=33\%\right)$ with a slight performance improvement by adopting the scheme $\mathbf{B}_J^{opt}$ with $I_{max} = 20$ instead of the scheme $\mathbf{B}_J^{comp\_1}$ with $I_{max} = 30$. Meanwhile, the iteration number affects the power consumption and throughput directly, which signifies that one can reduce power by nearly 33% and increase the throughput [16] by 50% $\left(\frac{1/20-1/30}{1/30}= 50\%\right)$ through using the scheme $\mathbf{B}_J^{opt}$ with $I_{max} = 20$ rather than the scheme $\mathbf{B}_J^{comp\_1}$ with $I_{max} = 30$.

In order to investigate the convergence speeds of the codes, the comparison of the averaged iteration numbers are shown in Fig. D2. From this figure, one can see that the average iteration number of $\mathbf{B}_J^{opt}$ is 12.5% and 13.9% lower at $E_b/N_0 = -0.5$dB, compared with $\mathbf{B}_J^{comp\_1}$ and $\mathbf{B}_J^{comp\_2}$, respectively. That is, the convergence speed of the proposed $\mathbf{B}_J^{opt}$ is the fastest. Table D1 lists the sums of entries of different PCMs of channel codes. In this table, $\mathbf{H}_{cc}^{opt}$, $\mathbf{H}_{cc}^{comp\_1}$ and $\mathbf{H}_{cc}^{comp\_2}$, are the PCMs of $\mathbf{B}_{cc}^{opt}$, $\mathbf{B}_{cc}^{comp\_1}$ and $\mathbf{B}_{cc}^{comp\_2}$, respectively. From this table, it can be seen that the sum of the entries of the proposed $\mathbf{H}_{cc}^{opt}$ is 120 and 40 less than $\mathbf{H}_{cc}^{comp\_1}$ and $\mathbf{H}_{cc}^{comp\_2}$, which reduce 120 and 40 edge arithmetic operations respectively when $\mathbf{H}_{cc}^{opt}$ is adopted. The longer the code length, the more the arithmetic operations can be reduced. It also means that the sum of entries in $\mathbf{H}_J^{opt}$ is the smallest. Since $\mathbf{H}_J^{opt}$ has both the minimum number of iterations and the smallest sum of the entries, it has the lowest decoding complexity.

Appendix D.2 Performance Comparisons over Rayleigh Fading Channel

Fig. D3 shows the BER performance of $\mathbf{B}_J^{opt}$ over Rayleigh fading channel at $p_m = 0.04$ when $I_{max} = 20$. From this figure, it can be seen that $\mathbf{B}_J^{opt}$ can achieve 0.58dB and 0.56dB coding gains, compared with $\mathbf{B}_J^{comp\_1}$ at $BER = 4 \times 10^{-7}$ and $\mathbf{B}_J^{comp\_2}$ at $BER = 1 \times 10^{-6}$, respectively. The performance improvement of the proposed $\mathbf{B}_J^{opt}$ over Rayleigh fading channel is more prominent than AWGN channel, and this also shows that the proposed $\mathbf{B}_J^{opt}$ can perform well over both Rayleigh fading channel and AWGN channel.

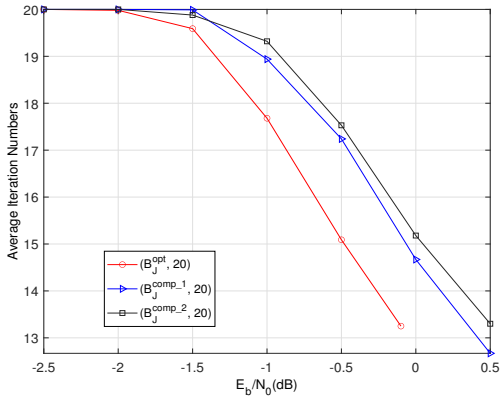

Figure D2 Comparison of average numbers of iterations at $p_m = 0.04$ over AWGN channel.

Table D1 Comparison of Sums of the Entries in $\mathbf{H}_{cc}$.

	H_{cc}^{opt}	$\boldsymbol{H_{cc}^{comp\_1}}$ [10]	$\boldsymbol{H_{cc}^{comp\_2}}$ [10]
$Sum(\mathbf{H}_{cc})$	1000	1120	1040

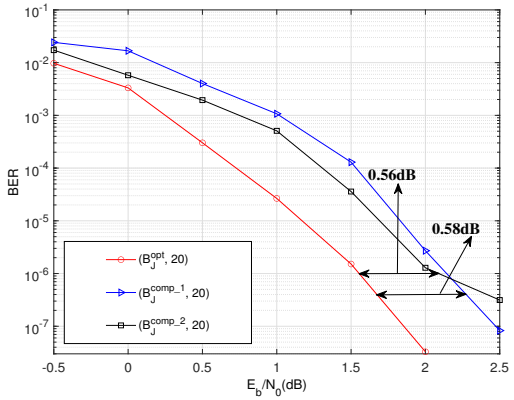

Figure D3 BER performance comparison at $p_m = 0.04$ over Rayleigh fading channel.

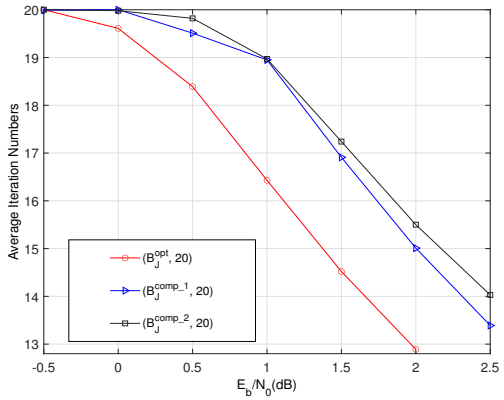

Figure D4 Comparison of average numbers of iterations at $p_m = 0.04$ over Rayleigh fading channel.

A comparison of the averaged iteration numbers over Rayleigh fading channel at $p_m = 0.04$ when $I_{max} = 20$ is shown in Fig. D4. When $E_b/N_0 = 2$dB, the averaged iteration number of $\mathbf{B}_J^{opt}$ is reduced up to 14.1% and 16.8%, compared with $\mathbf{B}_J^{comp\_1}$ and $\mathbf{B}_J^{comp\_2}$, respectively. The proposed $\mathbf{B}_J^{opt}$ can converges fastest among them over both AWGN channel and Rayleigh fading channel.

References

1 M. Fresia, F. Perez-Cruz, H. V. Poor, and S. Verdu, "Joint source and channel coding," *IEEE Signal Process. Mag.*, vol. 27, pp. 104–113, Nov. 2010.

2 X. Chen, "Zero-delay Gaussian joint source-channel coding for the interference channel," *IEEE Commun. Lett.*, vol. 22, no. 4, pp. 712–715, Nov. 2018.

3 C. Y. Bi, and J. Liang, "Joint source-channel coding of JPEG 2000 image transmission over two-way multi-relay networks," *IEEE Trans. Image Process.*, vol. 26, no. 7, pp. 3594–3608, Jul. 2017.

4 C. Chen, L. Wang and S. Liu, "The design of protograph LDPC codes as source codes in a JSCC system," *IEEE Commun. Lett.*, vol. 22, no. 4, pp. 672–675, Apr. 2018.

5 J. He, Y. Li, G. Wu, S. Qian, Q. Xue and T. Matsumoto, "Performance improvement of joint source-channel coding with unequal power allocation," *IEEE Wireless Commun. Lett.*, vol. 6, no. 5, pp. 582–585, Oct. 2017.

6 Q. Chen, L. Wang, S. Hong and Z. Xiong,"Performance improvement of JSCC scheme through redesigning channel code," *IEEE Commun. Lett.*, vol. 20, no. 6, pp. 1088–1091, Jun. 2016.

7 S. Hong, Q. Chen and L. Wang, "Performance analysis and optimisation for edge connection of JSCC system based on double protograph LDPC codes," *IET Communications*, vol. 12, no. 2, pp. 214–219, Jan. 2018.

8 S. Liu, C. Chen, L. Wang and S. Hong, "Edge connection optimization for JSCC system based on DP-LDPC codes," *IEEE Wireless Commun. Lett.*, vol. 8, no. 4, pp. 996–999, Aug. 2019.

9 C. Chen, L. Wang and F. C. M. Lau, "Joint optimization of protograph LDPC code pair for joint source and channel coding," *IEEE Trans. Commun.*, vol. 66, no. 8, pp. 3255–3267, Aug. 2018.

10 S. Liu, L. Wang, J. Chen and S. Hong, "Joint component design for the JSCC system based on DP-LDPC codes," *IEEE Trans. Commun.*, vol. 68, no. 9, pp. 5808–5818, Sept. 2020.

11 Q. Chen, L. Wang, S. Hong and Y. Chen, "Integrated design of JSCC scheme based on double protograph LDPC codes system," *IEEE Commun. Lett.*, vol. 23, no. 2, pp. 218–221, Feb. 2019.

12 Q. Chen and L. Wang, "Design and analysis of joint source channel coding schemes over non-standard coding channels," *IEEE Trans. Veh. Technol.*, vol. 69, no. 5, pp. 5369–5380, May 2020.

13 G. Cai, Y. Fang, P. Chen, G. Han, G. Cai and Y. Song, "Design of an MISO-SWIPT aided code-index modulated multi-carrier M-DCSK system for e-health IoT," *IEEE J. Sel. Areas Commun.*, vol. 39, no. 2, pp. 1–14, Feb. 2021.

14 T. J. Richardson, M. A. Shokrollahi and R. L. Urbanke, "Design of capacity-approaching irregular low-density parity-check codes," *IEEE Trans. Inf. Theory*, vol. 47, no. 2, pp. 619–637, Feb. 2001.

15 I. P. Mulholland, E. Paolini, and M. F. Flanagan, "Design of protographbased LDPC code ensembles with fast convergence properties," in *Proc. IEEE SCC*, Feb. 2017, pp. 1-6.

16 C. Tang, M. Jiang, C. Zhao and H. Shen, "Design of protograph-based LDPC codes with limited decoding complexity," *IEEE Commun. Lett.*, vol. 21, no. 12, pp. 2570–2573, Dec. 2017.

17 B. Smith, M. Ardakani, W. Yu, and F. R. Kschischang, "Design of irregular LDPC codes with optimized performance-complexity tradeoff," *IEEE Trans. Commun.*, vol. 58, no. 2, pp. 489–499, Feb. 2010.

18 T. Kim and J. Heo, "Information-propagation-based scheduling for the fast convergence of shuffled decoding," *IEEE Commun. Lett.*, vol. 22, no. 7, pp. 1314–1317, Jul. 2018.

19 Z. Xu, L. Wang, S. Hong, F. C. M. Lau and C. Sham, "Joint shuffled scheduling decoding algorithm for DP-LDPC codes-based JSCC systems," *IEEE Wireless Commun. Lett.*, vol. 8, no. 6, pp. 1696–1699, Dec. 2019.

20 T. V. Nguyen, A. Nosratinia, and D. Divsalar, "The design of rate-compatible protograph LDPC codes," *IEEE Trans. Commun.*, vol. 60, no. 10, pp. 2841–2850, Oct. 2012.

21 L. Dai, Y. Fang, Z. Yang, P. Chen, Y. Li, "Protograph LDPC-coded BICM-ID with irregular CSK mapping in visible light communication systems," *IEEE Trans. Veh. Technol.*, vol. 70, no. 10, pp. 11033–11038, Oct. 2021.

22 P. Chen, K. Cai and S. Zheng, "Rate-adaptive protograph LDPC codes for multi-level-cell NAND flash memory," *IEEE Commun. Lett.*, vol. 22, no. 6, pp. 1112–1115, Jun. 2018.

23 Q. Chen, L. Wang, P. Chen and G. Chen, "Optimization of component elements in integrated coding systems for green communications: a survey," *IEEE Commun. Surveys Tuts.*, vol. 21, no. 3, pp. 2977–2999, 3rd Quart., 2019.

24 G. Liva and M. Chiani, "Protograph LDPC codes design based on EXIT analysis," in *Proc. IEEE GLOBECOM*, Nov. 2007, pp. 3250–3254.

25 X.-Y. Hu, E. Eleftheriou, and D. M. Arnold, "Regular and irregular progressive edge-growth tanner graphs," *IEEE Trans. Inf. Theory*, vol. 51, no. 1, pp. 386–398, Jan. 2005.

26 J. Hou, P. H. Siegel, and L. B. Milstein, "Performance analysis and code optimization of low density parity-check codes on Rayleigh fading channels," *IEEE. J. Sel. Areas Commun.*, vol. 19, no. 5, pp. 924–934, May 2001.

27 H. Mukhtar, A. Al-Dweik and A. Shami, "Turbo product codes: Applications, challenges, and future directions," *IEEE Commun. Surveys Tuts.*, vol. 18, no. 4, pp. 3052–3069, 4th Quart., 2016.

28 D. Song, L. Wang, Z. Xu and G. Chen, "Joint code rate compatible design of DP-LDPC code pairs for joint source channel coding over implant-to-external channel," *IEEE Trans. Wireless Commun.*, vol. 21, no. 7, pp. 5526–5540, Jul., 2022.

29 C. Chen, Q. Chen, L. Wang, Y. -C. He and Y. Chen, "Probabilistic shaping for protograph LDPC-Coded modulation by residual source redundancy," *IEEE Trans. Commun.*,, vol. 69, no. 7, pp. 4267–4281, Jul., 2021.

30 Z. Xu, L. Wang and G. Chen, "Joint coding/decoding optimization for DC-BICM system: Collaborative design," *IEEE Commun. Lett.*, vol. 25, no. 8, pp. 2487–2491, Aug. 2021.